Journal of Zhejiang University SCIENCE A
ISSN 1009-3095 (Print); ISSN 1862-1775 (Online)
www.zju.edu.cn/jzus; www.springerlink.com
E-mail: jzus@zju.edu.cn

Influence of surface treatments on fatigue life of a two-stroke free piston linear engine component using random loading

RAHMAN M.M.†, ARIFFIN A.K.†, JAMALUDIN N., HARON C.H.C.

(*Department of Mechanical and Materials Engineering, Faculty of Engineering, Universiti Kebangsaan Malaysia, 43600 UKM, Bangi, Selangor DE, Malaysia*)

†E-mail: mustafiz@eng.ukm.my; kamal@eng.ukm.my

Received Feb. 20, 2006; revision accepted July 6, 2006

Abstract: This paper describes the finite element (FE) analysis technique to predict fatigue life using the narrow band frequency response approach. The life prediction results are useful for improving the component design methodology at the very early development stage. The approach is found to be suitable for a periodic loading but requires very large time records to accurately describe random loading processes. This paper is aimed at investigating the effects of surface treatments on the fatigue life of the free piston linear engine's components. Finite element modelling and frequency response analysis were conducted using computer aided design and finite element analysis commercial codes, respectively. In addition, the fatigue life prediction was carried out using finite element based fatigue analysis commercial code. Narrow band approach was specially applied to predict the fatigue life of the free piston linear engine cylinder block. Significant variation was observed between the surface treatments and untreated cylinder block of free piston engine. The obtained results indicated that nitrided treatment yielded the longest life. This approach can determine premature products failure phenomena, and therefore can reduce time to market, improve product reliability and customer confidence.

Key words: Vibration fatigue, Finite element (FE), Power spectral density function, Frequency response, Surface treatment
doi:10.1631/jzus.2006.A1819 **Document code:** A **CLC number:** TB114.3

INTRODUCTION

Fatigue durability has long been important issues in the design of a two-stroke free piston linear engine structure (Torres and Voorwald, 2002; Rahman *et al*., 2005a; 2005b). Durability assessment is traditionally done in the later part of the product development stage when prototypes are available, and heavily relied on in confirming ground durability tests. This process is very time consuming and often results in over-design with weight penalties, which is the major obstacle to achieve fuel economy. Due to the development of computer-aided engineering (CAE) tools, a three steps process including multibody dynamic analysis, finite element analysis, and fatigue life prediction, is more often used nowadays for early product durability evaluation (Rahman *et al*., 2005a; 2005b; Baek *et al*., 1993; Kuo and Kelkar, 1995a; 1995b; Kim *et al*., 2002). This approach helps the design engineer collect necessary information for continuous design analysis, and predict the durability of the free piston linear generator engine in the early design stage, thereby eliminating some of the shortcomings in the traditional durability evaluation method. Rahman and Ariffin (2005), and Rahman *et al*.(2005c; 2005d; 2005e) carried out the finite element based vibration fatigue analysis techniques to predict the fatigue life of free piston engine component using random load. Rahman *et al*.(2005f; 2005g) also presented finite element based fatigue life prediction of the free piston engine components under variable amplitude loading conditions using total-life

* Project (No. 03-02-02-0056 PR0025/04-03) supported by the Intensification of Research in Priority Areas (IRPA), Ministry of Science, Technology and Innovation, Malaysia

and crack initiation approaches.

Fatigue is a great concern for components subject to cyclic stresses, particularly where safety is paramount, as in the components of free piston linear engine. It has long been recognized that fatigue cracks generally start from free surfaces and that performance is therefore dependent on the surface topology/integrity produced by surface finishing. It is well known that in service, many more components and structures fail due to cyclic instead of static loading. The failure by fracture depends on a large number of parameters and is very often developed from particular surface areas of engineering components. Therefore, it is possible to improve the fatigue strength of engineering components by suitable surface treatments. Nowadays, manufacturers are utilizing different surface treatments to enhance the surface properties of engineering materials. So far, there are various methods employed to improve the fatigue strength, including optimization of geometric design parameters, materials and surface processing such as nitriding, cold rolling, shot peening, etc. (Rodopoulos *et al*., 2004).

Light metals have been utilized to produce automotive parts to reduce the weight of automobiles, aiming at significant reduction of CO_2 emission and environmental burdens (Boms and Whitacre, 2005; Vissutipitukul and Aizawa, 2005). The use of aluminum (Al) to replace steel for lightening of vehicle components or machine parts has recently increased. Al and its alloys have advantages over non metallic materials: aluminum alloys have a high melting point, good corrosion resistance, good workability and high thermal conductivity. However, the hardness and wear resistance of Al alloys are respectively lower and inferior to those of steel. Therefore, there is a limitation in their application for moving parts. So research has been carried out in surface modification technology to increase the applicability of Al alloys as moving parts. Surface modification technologies for Al alloys can be classified into three main categories namely alloying, coating and heat-treating process (Tomida and Nakata, 2003; Okumiya *et al*., 2001; 2005; Tsunekawa *et al*., 2003; Takeuchi *et al*., 2004).

The principal surface treatments such as carburizing or carbonitriding are preferred for many mechanical components before their delivery. These treatments are aimed at differentiating the response of surface and core to external loading by changing the surface material properties and by introducing appropriate residual stress distribution in order to improve their fatigue and wear behaviour (Benedetti *et al*., 2002). Different treatments can be carried out to locally improve the material response and to modify the stress field. A combination of case hardening followed by nitriding, and shot peening seems to give interesting results (Inoue *et al*., 1989). Shot peening process followed by case hardening can improve the microstructure and residual stress distribution of the components. Usually, residual stresses are introduced by shot peening because of the intense plastic deformation in the surface region (Kobayashi *et al*., 1998). Depending on whether the plastic deformation takes place on or below the surface, a shift of the residual stress peaks can be observed with respect to the surface.

Residual stresses can greatly improve the service life of many mechanical parts because they generally have some beneficial effects on the fatigue strength and corrosion resistance. Nowadays, many mechanical manufacturers consider the residual stress state as a quality parameter to be controlled. Whatever the types of mechanical treatment (shot peening, rolling, or machining), thermochemical (nitriding or carburizing), or thermal (quenching), residual stresses are always produced by the strain misfits or local material behavior differences. In each case, the exposure of the treated components in the recovery temperature range activates some microstructural mechanisms that lower the internal energy stored in the affected layers (Lillamand *et al*., 2000).

This work is aimed at investigating the influence of surface treatments on the high cycle fatigue of a vibrating aluminum alloys cylinder block of a two-stroke free piston engine. These investigations are essential in order to understand the involvement of microstructural mechanisms of hardening or softening due to service load. Numerical investigations were done to characterize completely the different induced effects before and after surface treatments. The numerical results are discussed and analyzed.

THE SPECTRAL MOMENTS FROM THE POWER SPECTRAL DENSITY FUNCTION

The stress power spectra density represents the frequency domain approach input into the fatigue

analysis (Bishop and Sherratt, 2000; MSC, 2004). This is a scalar function that describes how the power of the time signal is distributed among frequencies (Bendat, 1964). Mathematically this function can be obtained using a Fourier transform of the stress time history's auto-correlation function, and its area represents the signal's standard deviation. The power spectral density (PSD) is the most complete and concise representation of a random process. The statistical properties of a stationary ergodic process (Rahman *et al*., 2005c; Crandell and Mark, 1973; Newland, 1993; Wirsching *et al*., 1995) can be computed from a single time history with sufficiently long period. The time average of a random variable $x(t)$ is equal to the expected value of $x(t)$, as defined by

$$E[x(t)]=\int_{-\infty}^{\infty}x(t)\,\mathrm{d}t. \tag{1}$$

The mean square value of $x(t)$ is

$$E[x^2(t)]=\int_{-\infty}^{\infty}x^2(t)\,\mathrm{d}t.$$

Correlation function is a measure of the similarity between two random quantities in a time domain τ. For a single record $x(t)$, the autocorrelation $R(\tau)$ of $x(t)$ is the expected value of the product $x(t)x(t+\tau)$:

$$R(\tau)=E[x(t)x(t+\tau)]=\int_{-\infty}^{\infty}x(t)x(t+\tau)\,\mathrm{d}t. \tag{2}$$

When τ=0, the definition Eq.(2) reduces to the mean square value:

$$R(0)=E[x^2(t)].$$

For two random quantities $x(t)$ and $y(t)$, the cross correlation function is defined as

$$R_{xy}(\tau)=E[x(t)y(t+\tau)],\ R_{yx}(\tau)=E[y(t)x(t+\tau)]. \tag{3}$$

Then, the autocorrelation function is defined as with a time separation, τ

$$R_{xx}(\tau)=\int_{-\infty}^{\infty}x(t)x(t+\tau)\mathrm{d}t=E[x(t)x(t+\tau)].$$

The autocorrelation and PSD functions are related by the Fourier transform pair

$$S_{xx}(\omega)=\frac{1}{2\pi}\int_{-\infty}^{\infty}R_{xx}(\tau)\mathrm{e}^{-\mathrm{j}\omega\tau}\mathrm{d}\tau, \tag{4}$$

$$R_{xx}(\tau)=\int_{-\infty}^{\infty}S_{xx}(\omega)\mathrm{e}^{\mathrm{j}\omega\tau}\mathrm{d}\omega. \tag{5}$$

As S_{xx} is a real even valued function

$$R_{xx}(\tau)=\int_{-\infty}^{\infty}S_{xx}(\omega)\cos\omega\tau\mathrm{d}\omega, \tag{6}$$

by differentiating $R_{xx}(\tau)$ several times with respect to τ, the following equations are obtained

$$R'_{xx}(\tau)=R_{x\dot{x}}(\tau)=-\int_{-\infty}^{\infty}\omega S_{xx}(f)\sin\omega\tau\,\mathrm{d}f, \tag{7}$$

$$R''_{xx}(\tau)=-R_{\dot{x}\dot{x}}(\tau)=-\int_{-\infty}^{\infty}\omega^2 S_{xx}(f)\cos\omega\tau\,\mathrm{d}f, \tag{8}$$

$$R'''_{xx}(\tau)=-R_{\ddot{x}\dot{x}}(\tau)=\int_{-\infty}^{\infty}\omega^3 S_{xx}(f)\sin\omega\tau\,\mathrm{d}f, \tag{9}$$

$$R''''_{xx}(\tau)=R_{\ddot{x}\ddot{x}}(\tau)=\int_{-\infty}^{\infty}\omega^4 S_{xx}(f)\cos\omega\tau\,\mathrm{d}f. \tag{10}$$

The moments therefore, define how each of the processes x, x', x'', etc. are related to the other processes, when τ=0,

$$\mu_n=\frac{\mathrm{d}^n}{\mathrm{d}\tau^n}R_{xx}(0)=\frac{\mathrm{d}^n}{\mathrm{d}t^n}R_{xx}(0)=\int_{-\infty}^{\infty}\omega^n S_{xx}(f)\mathrm{d}f, \tag{11}$$

or in terms of the one sided PSD $G(f)$

$$\mu_n=\int_0^{\infty}(2\pi f)2S_{xx}(f)\mathrm{d}f=(2\pi)^n\int_0^{\infty}f^nG_{xx}(f)\,\mathrm{d}f=m_n(2\pi)^n, \tag{12}$$

where $m_n=\int_0^{\infty}f^nG_{xx}(f)\,\mathrm{d}f$.

The method for computing these moments is shown in Fig.1.

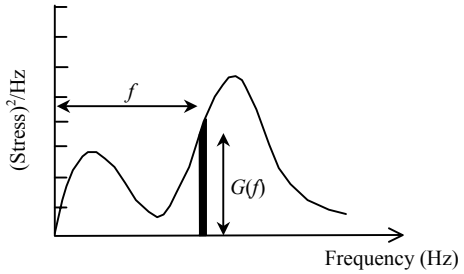

Fig.1 Calculating moments from a PSD

It is important to note that μ_1 and μ_3 are zero, but that m_1 and m_3 are not. Remember that μ_n is produced by integrating from $-\infty$ to $+\infty$, and m_n is produced by integrating from 0 to $+\infty$. Typically, we calculate m_0, m_1, m_2, and m_4.

The most common spectral moment is μ_0, which determines the variance of a PSD

$$\mu_0=\sigma_x^2=\int_{-\infty}^{\infty}S_{xx}(\omega)\mathrm{d}\omega=2\int_0^{\infty}S_{xx}(\omega)\mathrm{d}\omega=\int_0^{\infty}G(f)\mathrm{d}f=m_0. \tag{13}$$

here, μ_0 and m_0 are equal. The root mean square (RMS) value of the zero mean process is given by $\sqrt{m_0}$.

A more complicated example of the use of these moments considers the number of zero crossings in a stationary random and Gaussian (normal) process. Consider the following 2D probability function $p(\alpha,\beta)$ of x and $\dot{x}$

$$p(\alpha,\beta)\Delta\alpha\Delta\beta\approx\mathrm{Prob}[\alpha\le x(t)\le\alpha+\Delta\alpha \text{ and } \beta\le\dot{x}(t)\le\beta+\Delta\beta]. \tag{14}$$

This probability represents the fraction of time that x is between α and $\Delta\alpha$, while the velocity $\dot{x}$ is between $\beta+\Delta\beta$. If we define the time to cross one interval as Δt,

$$\Delta t=\Delta\alpha/|\beta|, \tag{15}$$

then we can obtain the expected total number of positive crossings of level as

$$\frac{p(\alpha,\beta)\Delta\alpha\Delta\beta}{\Delta t}\approx|\beta|\,p(\alpha,\beta)\Delta\beta. \tag{16}$$

As $\Delta\beta\to0$, the total expected number of passages per unit time through $x(t)=\alpha$ for all possible values of β is given by

$$E[\alpha]=\int_0^{\infty}|\beta|p(\alpha,\beta)\mathrm{d}\beta. \tag{17}$$

By setting $\alpha=0$, we get the required number of zero crossings per unit time

$$E[0]=\int_0^{\infty}|\beta|\,p(0,\beta)\mathrm{d}\beta. \tag{18}$$

The 2D normal density function of x and $\dot{x}$ is given by

$$p(\alpha,\beta)=(2\pi)^{-1}|\boldsymbol{A}|^{-0.5}\,\mathrm{e}^{\left[\frac{-1}{2|\boldsymbol{A}|}(A_{11}\alpha^2+2A_{12}\alpha\beta+A_{22}\beta^2)\right]}, \tag{19}$$

where

$$\boldsymbol{A}=\begin{bmatrix}a_{11}&a_{12}\\a_{21}&a_{22}\end{bmatrix} \text{ and } a_{ij}=E[x_ix_j]=a_{ji}. \tag{20}$$

The a_{ij} terms are the covariances or second moments of x_i and x_j. The a_{ii} terms are the variances of x_i and x_i. $|\boldsymbol{A}|$ is the determinant of $\boldsymbol{A}$ and A_{ij} is the cofactor of a_{ij}.

With a little effort, we get

$$a_{11}=R(0)=\mu_0,\ a_{12}=a_{21}=\mu_1=0,\ a_{22}=\mu_2. \tag{21}$$

Therefore,

$$\boldsymbol{A}=\begin{bmatrix}\mu_0&0\\0&\mu_2\end{bmatrix}.$$

Then we get,

$$E[\alpha]=\frac{1}{2\pi}[\mu_2/\mu_0]^{1/2}\,\mathrm{e}^{\frac{\alpha^2}{2\mu_0}}. \tag{22}$$

If we set $\alpha=0$, then $E[0]=[m_2/m_0]^{1/2}$.

Similarly, the number of peaks per unit time is $E[P]=[m_4/m_2]^{1/2}$.

The irregularity factor is $\gamma=E[0]/E[P]=[m_2/\sqrt{m_0m_4}\,]$.

The irregularity factor γ is an important parameter that can be used to evaluate the concentration of the process near a central frequency. Therefore, γ can be used to determine whether the process is narrow band or wide band. A narrow band process ($\gamma\to1$) is characterized by only one predominant central frequency indicating that the number of peaks per second is very similar to the number of zero crossings of the signal. This assumption leads to the fact that the probability density function (pdf) of the fatigue cycles range is the same as the pdf of the peaks in the signal (Bendat theory). In this case the fatigue life is easy to estimate. In contrast, the same property is not true for wide band process ($\gamma\to0$). Fig.2 shows different types of time histories with corresponding PSD function.

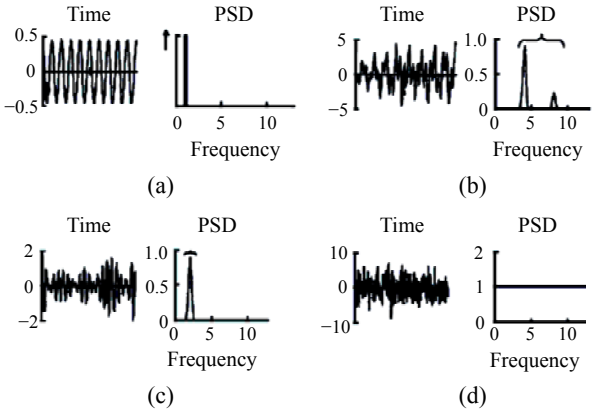

Fig.2 Equivalent time histories and PSDs. (a) Sine wave; (b) Broad band process; (c) Narrow band process; (d) White noise process

PROBABILITY DENSITY FUNCTIONS

The most convenient way of storing stress range histogram information is in the form of a probability density function (pdf) of stress ranges (Rahman *et al*., 2005c; Bendat, 1964). A typical representation of this function is shown in Fig.3. It is very easy to transform the stress range histogram to pdf form, or backward. The bin widths used, and the total number of cycles recorded in the histogram are the only additional pieces of information required. To get a pdf from a rainflow histogram, each bin in the rainflow count has to be multiplied by S_tdS, where S_t is the total number of cycles in the histogram and dS is the interval width.

The probability of the stress range occurring between S_i–dS/2 and S_i+dS/2 is given by $p(S_i)$dS.

The actual counted number of cycles is equal to n_i=S_t[p(S)dS].

The allowable number of cycles is given by $N(S_i)$=k/S^b.

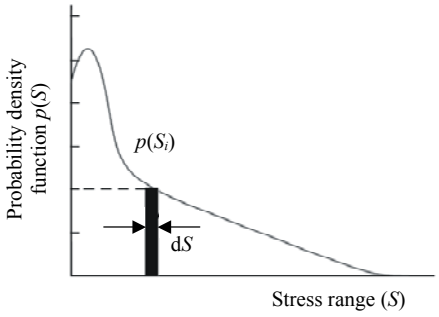

Fig.3 Probability density functions

The damage is then defined by

$$E[D]=\sum_i \frac{n_i}{N(S_i)}=\frac{S_t}{k}\int S^b p(S)\mathrm{d}S. \qquad (23)$$

Failure occurs if D≥1.0.

In order to compute fatigue damage over the lifetime of the structure in seconds, the form of materials S-N data must also be defined using the parameters k and b. The typical S-N curve is shown in Fig.4 which simply shows that under constant amplitude cyclic loading, a linear relationship exists between cycles to failure (N) and applied stress range (S) when plotted on log-log paper. There are two alternative ways to define this relationship, as given in Eq.(24). In addition, the total number of cycles in time T must be determined from the number of peaks per second E[P]. If the damage caused in time T is greater than 1.0 then the structure is assumed to have failed or alternatively the fatigue life can be obtained by setting E[D]=1.0 and then finding the fatigue life T in seconds from the fatigue damage as given by Eq.(24):

$$N = kS^{-b}, \text{ where } b=-1/b1, \text{ and } k=(SRI1)^b. \quad (24)$$

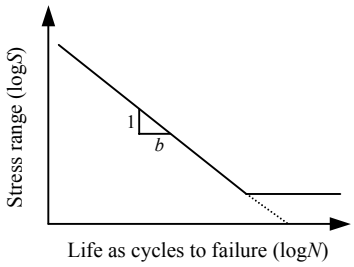

Fig.4 A typical *S*-*N* curve

NARROW BAND SOLUTION

Bendat (1964) proposed first significant step towards a method for determining fatigue life from PSDs which is the so-called narrow band solution and showed that the probability density function (pdf) of peaks for a narrow band signal tended towards Rayleigh distributions as the bandwidth reduced. Furthermore, for a narrow band time history, Bendat assumed that corresponding troughs of similar magnitude regardless of whether they actually formed

stress cycles would follow all the positive peaks in the time history. Using this assumption the pdf of stress range would also tend to Rayleigh distribution. To complete the solution method, Bendat used a series of equations derived by Rice (1954) to estimate the expected number of peaks using moments of area beneath the PSD. The narrow band solution (Rahman *et al*., 2005c; Bishop and Sherratt, 2000) for the range mean histogram is therefore expressed by Eq.(25):

$$E[D]=\sum_i \frac{n_i}{N(S_i)}=\frac{S_t}{K}\int S^b p(S)\mathrm{d}S$$
$$=\frac{E[P]T}{K}\int S^b\left(\frac{S}{4m_0}\mathrm{e}^{S^2/(8m_0)}\right)\mathrm{d}S=E[P]T\left\{\frac{S}{4m_0}\mathrm{e}^{S^2/(8m_0)}\right\}. \quad (25)$$

This is the first frequency domain method for predicting fatigue damage from PSDs assuming that the pdf of the peaks is equal to the pdf of the stress amplitudes. The narrow band solution was then obtained by substituting the Rayleigh pdf of peaks with the pdf of stress ranges. The full equation is obtained by noting that S_t is equal to $E[P]T$, where T is the life of the structure in seconds. The basis of the narrow band solution is shown in Fig.5.

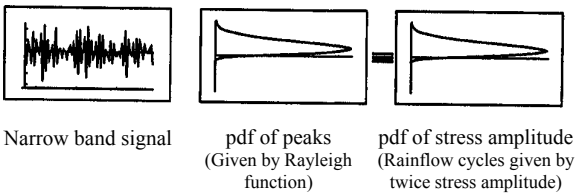

Fig.5 The Basis of the narrow band solution (Bishop and Sherratt, 2000)

APPLICATION OF FREE PISTON LINEAR ENGINE COMPONENT

Finite element modelling

A geometric model of the free piston engine's cylinder block is considered in this study. There are several contact areas including cylinder head, gasket, hole for bolt. Therefore, constraints are employed for the following purposes: (1) to specify the prescribed enforced displacements, (2) to simulate the continuous behavior of displacement in the interface area, and (3) to enforce rest condition in the specified directions at grid points of reaction. 3D model of free piston linear engine cylinder block was developed using CATIA® software. A parabolic tetrahedral element was used for the solid mesh. Sensitivity analysis was performed to obtain the optimum element size. These analyses were performed iteratively for different element lengths until the solution yielded appropriate accuracy. Convergence of stresses was observed as the mesh size was successively refined. The element size of 0.20 mm was finally considered. A total of 35415 elements and 66209 nodes were generated with 0.20 mm element length. Compressive loads were applied as pressure (7 MPa) acting on the surface of the combustion chamber and preloads were applied as pressure (0.3 MPa) acting on the bolt-hole surfaces. In addition preload was also applied on the gasket surface generating pressure of 0.3 MPa. Multi-point constraints (MPCs) (Schaeffer, 2001) were applied on the bolt-hole for all six degrees of freedom and were used to connect the parts through the interface nodes. These MPCs were acting as an artificial bolt and nut that connects each part of the structure. Each of the MPCs will be connected using a Rigid Body Element (RBE) that indicates the independent and dependent nodes. The configuration of the engine is constrained by bolts to the cylinder head and the cylinder block. In the condition with no loading configuration the RBE element with six-degree of freedom was assigned to the bolts and the hole on the cylinder head. The independent node was created on the cylinder block hole. Due to the complexity of the geometry and loading on the cylinder block, a 3D finite element model (FEM) was adopted as shown in Fig.6. The loading, constraints and boundary conditions on the cylinder block are shown in Fig.7.

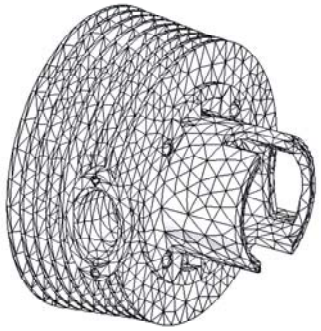

Fig.6 3D finite element model

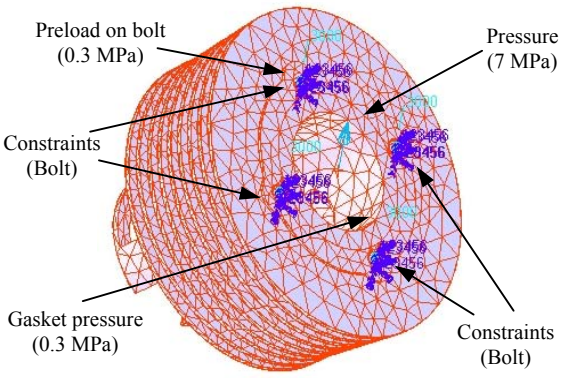

Fig.7 Loading, constraints and boundary conditions

Loading information

Several types of variable amplitude loading history were selected from the SAE and ASTM profiles for the FE based fatigue analysis. The detailed information about these histories is given in (Tucker and Bussa, 1977). The variable amplitude load-time histories are shown in Fig.8 and the corresponding PSD plots are also shown in Fig.9. The terms of SAETRN, SAESUS, and SAEBRAKT represent the load-time history for the transmission, suspension, and bracket respectively (Rahman *et al*., 2005c; Tucker and Bussa, 1977). The considered load-time histories are based on the SAE's profile. In addition, I-N, A-A, A-G, R-C, and TRANSP represent the ASTM instrumentation and navigation, ASTM air to air, ASTM air to ground, ASTM composite mission typical loading history, and ASTM composite mission typical transport loading history respectively (Rahman *et al*., 2005b; 2005c). The abscissa is the time in seconds.

Results and discussion

Frequency response analysis was conducted using MSC.NASTRAN finite element code. The frequency response analysis used damping ratio of 5% of critical damping. The damping ratio is the ratio of the actual damping in the system to the critical damping. Most experimental modal analysis software packages report the modal damping in terms of non-dimensional critical damping ratio expressed as a percentage (Formenti, 1999; Gade *et al*., 2002). In fact, most structures have critical damping values in the range of 0 to 10%, with values of 1% to 5% as the typical range

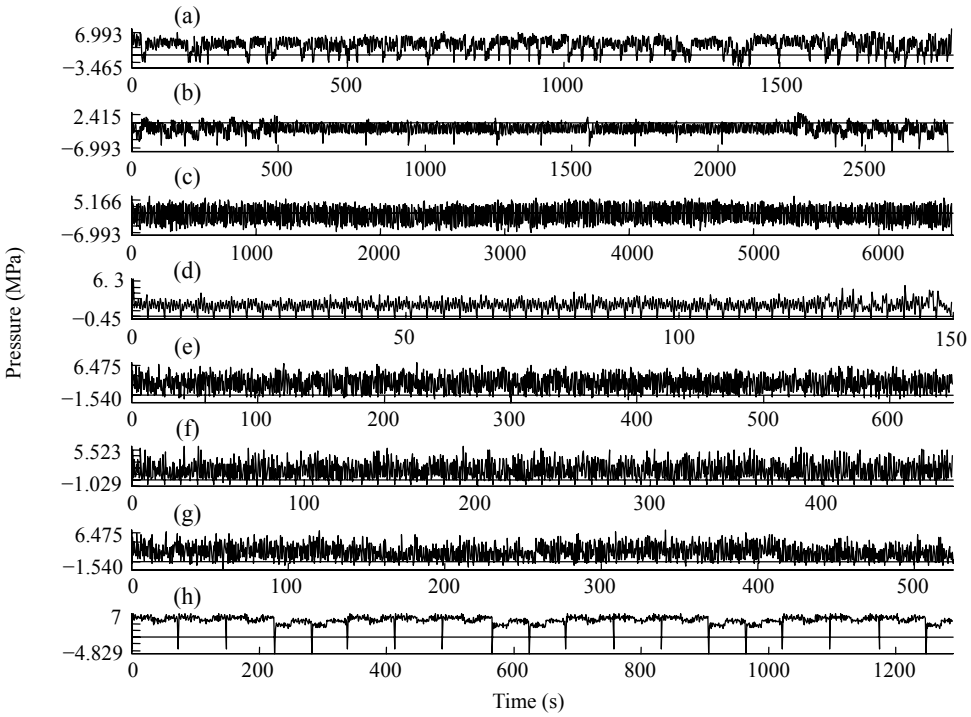

Fig.8 Different time loading histories. (a) SAE standard transmission (SAETRN) loading; (b) SAE standard suspension (SAESUS) loading; (c) SAE standard bracket (SAEBKT) loading; (d) ASTM instrumentation and navigation (I-N) typical loading; (e) ASTM air to air (A-A) typical loading; (f) ASTM air to ground typical loading; (g) ASTM composite mission (R-C) typical loading; (h) ASTM composite mission transport (TRANSP) typical loading

(BDA, 2002). Zero damping ratio indicates that the mode is undamped and one means it is critically damped. The results of Pseudo-static and frequency response finite element analysis at zero Hz i.e. the maximum principal stresses distribution of cylinder block are presented in Figs.10 and 11 respectively. From the results, the maximum and minimum principal stresses of 38.0 MPa and –7.75 MPa for Pseudo static analysis, and 38.0 MPa and –7.83 MPa for frequency response analysis at zero Hz were obtained respectively. These two contour plots are almost identical.

When the plots are drawn at higher frequencies, it can be shown that a small variation occurs in the static cases. This variation is due to the dynamic influences of the first mode shape. It can be seen that the maximum principal stress varies with higher frequencies. The variation of the maximum principal stresses with the frequency is shown in Fig.12 indicating that the maximum principal stress occurs at a frequency of 32 Hz.

The maximum principal stresses of the cylinder block for the frequency response analysis at 32 Hz is presented in Fig.13. From the results, the maximum and minimum principal stresses of 56.1 MPa at node 50420, and –20.7 MPa at node 47782 were obtained,

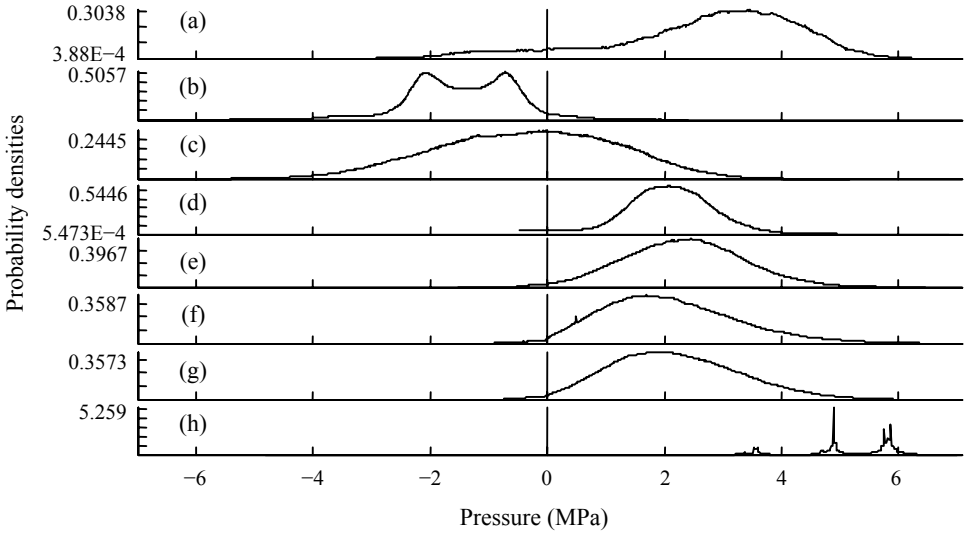

Fig.9 Power spectral densities (PSDs) responses. (a) SAE standard transmission (SAETRN) loading; (b) SAE standard suspension (SAESUS) loading; (c) SAE standard bracket (SAEBKT) loading; (d) ASTM instrumentation and navigation (I-N) typical loading; (e) ASTM air to air (A-A) typical loading; (f) ASTM air to ground typical loading; (g) ASTM composite mission (R-C) typical loading; (h) ASTM composite mission transport (TRANSP) typical loading

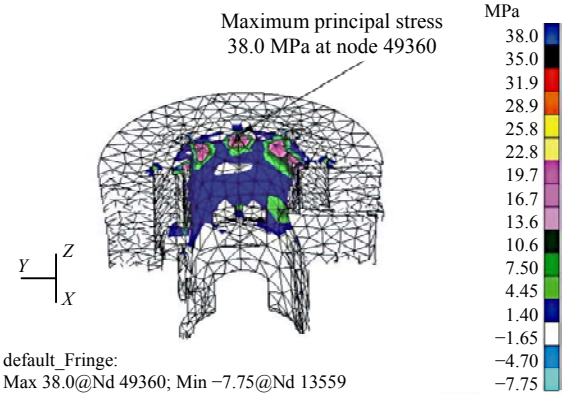

Fig.10 Maximum principal stresses distribution for linear static analysis

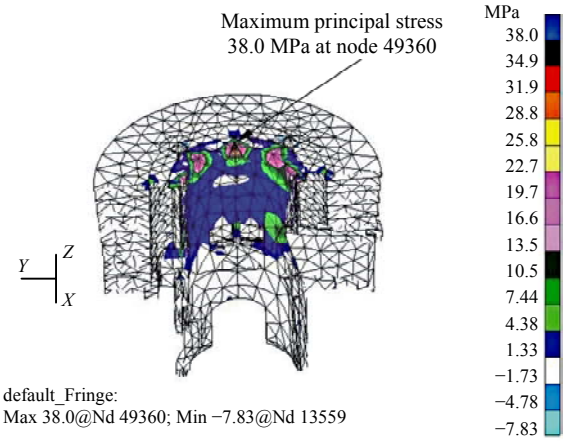

Fig.11 Maximum principal stresses distribution for frequency analysis at zero Hz

respectively. The fatigue life contour result for the most critical location for 32 Hz is shown in Fig.14 using the SAETRN loading histories (Rahman *et al*., 2005c). The minimum life prediction is $10^{9.44}$ s for 32 Hz. Table 1 shows the comparison between Pseudo-static and vibration fatigue analysis using narrow band frequency response method for different loading conditions of a cylinder block made of AA6061-T6 material. It is observed from Table 1 that there is a good agreement between the Pseudo-static and vibration fatigue analysis approaches. The full set of the comparison results for the untreated polished cylinder block at critical location (node 49360) is given in Table 2 with different loading conditions. The narrow band solution is considered in this study. It is observed that from Table 2, the SAESUS loading condition gives the longest life for all materials while ASTM A-G loading condition gives the shortest life for all materials.

The effect of surface treatments on the fatigue life of the component subjected to variable amplitude loading conditions was also investigated. The material used in this study was AA6061-T6 and the surface finish was in polished condition. A very high proportion of all the fatigue failures nucleate at the surface of components and therefore, the surface conditions become an extremely important factor in influencing the fatigue strength. Surface effects are caused by the differences in the surface roughness, microstructure, chemical composition, and residual stress (Bannantine *et al*., 1990). The correction factor for the surface finish is sometimes used as a qualitative description of the surface finish, such as polished or machined (Bannantine *et al*., 1990; Stephens *et al*., 2001). The surface factors are related to the ultimate tensile strength with different surface finish conditions such as grinding, machining, hot rolling, and forging (Juvinall and Marshek, 1991). The correction factors for surface treatment and finish are obtained

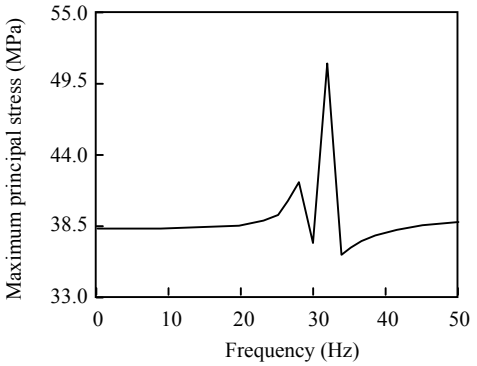

Fig.12 Maximum principal stresses plotted against frequency

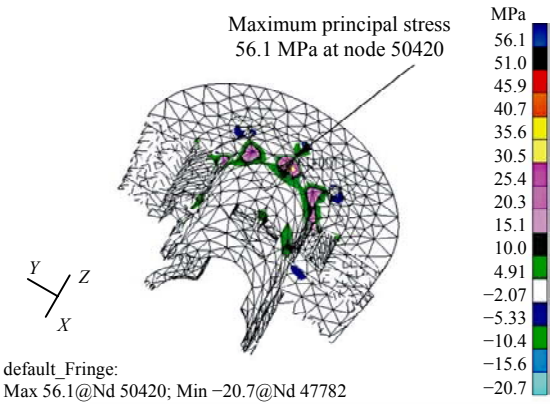

Fig.13 Maximum principal stresses contour for frequency response analysis at 32 Hz

Table 1 Predicted life in seconds between two approaches at critical location (node 49360)

Loading conditions	Pseudo-static approach	Vibration fatigue
SAETRN	1.14×10^{7}	2.10×10^{7}
SAESUS	6.34×10^{9}	8.74×10^{9}
SAEBKT	7.56×10^{7}	1.06×10^{8}
I-N	2.13×10^{8}	2.30×10^{8}
A-A	1.39×10^{7}	3.93×10^{7}
A-G	6.72×10^{6}	8.23×10^{6}
R-C	1.59×10^{7}	1.83×10^{7}
TRANSP	8.47×10^{8}	2.27×10^{9}

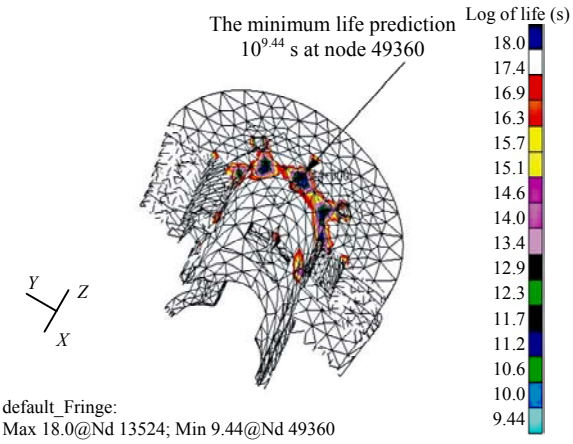

Fig.14 Vibration fatigue life in log contour plotted for 32 Hz

Table 2 Predicted life in seconds at weakest location (at node 49360)

Loading conditions	Predicted life in seconds at critical location (at node 49360)							
	2014-T6	2024-T86	2219-87	5083-87	5454-CF	6061-T6	7075-T6	7175-T73
SAETRN	4.27×10^{7}	1.25×10^{9}	8.48×10^{8}	3.56×10^{7}	1.30×10^{7}	2.10×10^{7}	1.08×10^{10}	2.33×10^{9}
SAESUS	5.01×10^{10}	3.78×10^{12}	3.36×10^{11}	2.51×10^{11}	9.24×10^{10}	8.74×10^{9}	9.51×10^{12}	1.10×10^{15}
SAEBKT	4.96×10^{8}	1.53×10^{10}	9.07×10^{9}	7.78×10^{8}	3.18×10^{8}	1.06×10^{8}	1.59×10^{11}	1.55×10^{11}
I-N	2.64×10^{8}	8.02×10^{9}	4.66×10^{9}	4.52×10^{8}	1.86×10^{8}	2.30×10^{8}	8.52×10^{10}	1.13×10^{11}
A-A	5.99×10^{7}	1.85×10^{9}	1.17×10^{9}	7.08×10^{7}	2.78×10^{7}	3.93×10^{7}	1.76×10^{10}	7.71×10^{9}
A-G	1.66×10^{7}	4.87×10^{8}	3.29×10^{8}	1.40×10^{7}	5.11×10^{6}	8.23×10^{6}	4.21×10^{9}	9.26×10^{8}
R-C	3.19×10^{7}	9.66×10^{8}	6.29×10^{8}	3.19×10^{7}	1.21×10^{7}	1.83×10^{7}	8.78×10^{9}	2.65×10^{9}
TRANSP	1.95×10^{9}	4.99×10^{10}	2.67×10^{10}	5.07×10^{9}	2.07×10^{9}	2.27×10^{9}	5.92×10^{11}	4.20×10^{12}

Table 3 Effect of surface treatments at different loading conditions for polished components

Loading conditions	Predicted life in seconds for different surface treatment processes			
	Nitrided	Cold rolled	Shot peened	Untreated
SAETRN	4.52×10^{10}	8.81×10^{8}	6.40×10^{7}	2.10×10^{7}
SAESUS	3.41×10^{6}	1.21×10^{14}	8.31×10^{11}	8.74×10^{9}
SAEBKT	8.08×10^{12}	5.31×10^{10}	1.68×10^{9}	1.06×10^{8}
I-N	6.35×10^{12}	3.68×10^{10}	1.01×10^{9}	2.30×10^{8}
A-A	2.77×10^{11}	2.92×10^{9}	1.40×10^{8}	3.93×10^{7}
A-G	1.84×10^{10}	3.51×10^{8}	2.52×10^{7}	8.23×10^{6}
R-C	7.21×10^{10}	1.02×10^{9}	6.01×10^{7}	1.83×10^{7}
TRANSP	2.40×10^{14}	9.55×10^{11}	1.33×10^{10}	2.27×10^{9}

from Lipton and Juvinall (1963), Juvinall and Marshek (1991) and Reemsnyder (1985) empirical data and are related to the ultimate strength of the material. The effects of the surface treatments on the fatigue lives under different loading conditions using the Narrow band frequency response method at critical location are summarized in Table 3.

Surface treatments including nitriding, cold rolling and shot peening that produced compressive residual surface stresses can prolong the fatigue life. These surface treatments cause the maximum tensile stress to occur below the surface of the materials. However, the tensile residual surface stresses are found to be very detrimental and can promote corrosion fatigue. In addition, surface treatments can also increase the endurance limit of the material used. A diffusion process such as nitriding is found to be very beneficial for increasing the fatigue strength. This process can increase the strength of the material on the surface as well as cause volumetric changes, which produce the residual compressive surface stresses. There are several available methods used to cool the surface of a component to produce a residual compressive stress. The two most important methods are cold rolling and shot peening. These methods are known to produce the compressive residual stresses and harden the surface material. The significant improvement in the fatigue life is due primarily to the generation of residual compressive stresses. In the shot peening process, the surface of the component undergoes plastic deformation due to the impact of many hard shots. The enhancing of the component fatigue life is due to the development of compressive residual stresses and the increase of hardness near the surface. The effect of surface treatment at different loading conditions for the polished vibrating cylinder block is summarized in Table 3. It is observed that the fatigue life for nitriding surface treatments is surprisingly higher than other surface treatment processes. Fig.15 shows the effect of different surface treatment processes for ASTM A-G loading conditions and polished specimen. It clearly indicates that nitrided processes produce the longest fatigue life at critical location (at node 49360, which produces the maximum stress and the longest life) compared to other processes.

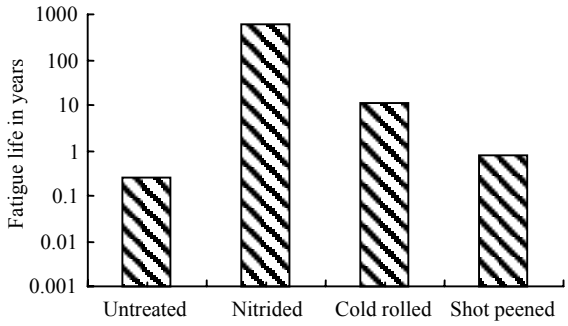

Fig.15 Effect of different surface treatment processes for polished and A-G loading conditions

CONCLUSION

The concept of spectral moments has been presented. The state-of-the-art of vibration fatigue techniques has been presented where the random loading and response are categorized using PSD functions. Narrow band frequency domain fatigue analysis has been applied to a typical cylinder block of a new two-stroke free piston engine. From the results, it can be concluded that the compressive mean stress-loading condition gives the longest fatigue life for all materials. The results clearly indicate that all the surface treatment processes can increase the fatigue life of aluminum alloys component. The surface residual compressive stress is found to have the greatest effect on the fatigue life. It can also be concluded that the combination of the polished and nitriding processes gives the longest life of the cylinder block. In addition, vibration fatigue analysis can improve understanding of the system behavior in terms of frequency characteristics of the structures, loads and their couplings.

ACKNOWLEDGMENT

The authors sincerely thank the Department of Mechanical and Materials Engineering, Faculty of Engineering, Universiti Kebangsaan Malaysia.

References

Baek, W.K., Stephens, R.I., Dopker, B., 1993. Integrated computational durability analysis. *Journal of Engineering for Industry, Transactions of the ASME*, **115**(4):492-499.

Bannantine, S.A., Comer, J.J., Handrock, J.L., 1990. Fundamentals of Metal Fatigue Analysis. Prentice-Hall, New Jersey, USA.

BDA (Basic Dynamic Analysis), 2002. User's Guide, MSC.Nastran Version 68. MSC.Software Corporation, USA.

Bendat, J.S., 1964. Probability Functions for Random Responses. NASA report on Contract NASA-5-4590.

Benedetti, M., Fortanari, V., Hohn, B.R., Oster, P., Tobie, T., 2002. Influence of shot peening on bending tooth fatigue limit of case hardened gears. *International Journal of Fatigue*, **24**(11):1127-1136. [doi:10.1016/S0142-1123(02)00034-8]

Bishop, N.W.M., Sherratt, F., 2000. Finite Element Based Fatigue Calculations. NAFEMS Ltd., UK.

Boms, R., Whitacre, D., 2005. Optimization Design of Aluminum Suspension Components Using an Integrated Approach. SAE Paper No. 95M-2.

Crandell, S.H., Mark, W.D., 1973. Random Vibration in Mechanical Systems. Academic Press, New York.

Formenti, D., 1999. The relationship between % of critical and actual damping in a structure. *Sound & Vibrations*, **33**(4):14-18.

Gade, S., Herlufsen, H., Konstantin-Hansen, H., 2002. How to determine the modal parameters of simple structures. *Sound & Vibrations*, **36**(1):72-73.

Inoue, K., Maehara, T., Yamanaka, M., 1989. The effect of Shot peening on the bending strength of carburized gear teeth. *JSME Inter. Journal Series III*, **32**(3):448-454.

Juvinall, R.C., Marshek, K.M., 1991. Fundamentals of Machine Component Design. John Willey and Sons, New York, USA.

Kim, H.S., Yim, H.J., Kim, C.B., 2002. Computational durability prediction of body structures in prototype vehicles. *International Journal of Automotive Technology*, **3**(4):129-135.

Kobayashi, M., Matsui, T., Murakami, Y., 1998. Mechanism of creation of compressive residual stress by shot peening. *International Journal of Fatigue*, **20**(5):351-357. [doi:10.1016/S0142-1123(98)00002-4]

Kuo, E.Y., Kelkar, S.G., 1995a. Vehicle Body Structure Durability Analysis. SAE Paper No. 951096.

Kuo, E.Y., Kelkar, S.G., 1995b. Body structure durability analysis. *Automotive Engineering*, **103**(7):73-77.

Lillamand, I., Barrallier, L., Sprauel, J.M., Chiron, R., 2000. Macroscopic and macroscopic evolutions of a shot peened layer during isothermal recovery. *Metallurgical and Materials Transactions A*, **31A**:213-219.

Lipson, C., Juvinall, R.C., 1963. Handbook of Stress and Strength: Design and Material Applications. Macmillan & Co., New York, USA.

MSC, 2004. MSC/FATIGUE User's Guide, Vol. 1 & 2. MSC/Corporation, USA.

Newland, D.E., 1993. An Introduction to Random Vibrations, Spectral and Wavelet Analysis. Longman Scientific and Technical, Essex, UK.

Okumiya, M., Tsunekawa, Y., Murayama, T., 2001. Surface modification of aluminum using ion nitriding and fluidize

bed. *Surface and Coatings Technology*, **142-144**:235-240. [doi:10.1016/S0257-8972(01)01151-3]

Okumiya, M., Tsunekawa, Y., Sugiyama, H., Tanaka, Y., Takano, N., Tomimoto, M., 2005. Surface modification of aluminum using ion nitriding and barrel nitriding. *Surface and Coatings Technology*, **200**(1-4):35-39. [doi:10.1016/j.surfcoat.2005.02.110]

Rahman, M.M., Ariffin, A.K., 2005. Vibration fatigue analysis of cylinder head of a new two-stroke free piston engine using finite element approach. *Journal of Structural Integrity and Durability*, **1**(2):121-129.

Rahman, M.M., Ariffin, A.K., Jamaluddin, N., Haron, C.H.C., 2005a. Fundamental Aspects of Finite Element Based Durability and Fatigue Analysis of Linear Generator Engine. Proceeding of the International Conference on Recent Advances in Mechanical and Materials Engineering (ICRAMME 2005), p.1105-1110.

Rahman, M.M., Ariffin, A.K., Jamaludin, N., Haron, C.H.C., 2005b. Modelling and Analysis of Cylinder Block of Linear Generator Engine for Fatigue Durability. Proceeding in the 4th International Conference on Numerical Analysis of Engineering (NAE-2005), Hotel SANTIKA, Yogyakarta, Indonesia, p.107-113.

Rahman, M.M., Ariffin, A.K., Jamaludin, N., Haron, C.H.C., 2005c. Analytical and Finite Element Based Fatigue Life Assessment of Vibration Induced Fatigue Damage. The Second International Conference on Research and Education in Mathematics (ICREM 2), Residence Hotel, Putrajaya, Malaysia, p.331-345.

Rahman, M.M., Ariffin, A.K., Jamaluddin, N., Haron, C.H.C., 2005d. Vibration Fatigue Analysis of Linear Generator Engine Using Frequency response Approach. Proceeding of the National Seminar on Advances in Malaysian Noise, Vibration and Comfort 2005 (NVC-2005), p.277-286.

Rahman, M.M., Ariffin, A.K., Jamaluddin, N., Haron, C.H.C., 2005e. Vibration Fatigue Analysis of a New Two-stroke Linear Generator Engine Using Finite Element Simulation. Proceedings of the National Seminar on Computational and Experimental Mechanics (CEM2005), p.259-267.

Rahman, M.M., Ariffin, A.K., Jamaluddin, N., Haron, C.H.C., 2005f. Prediction of Fatigue Life of Aluminum Alloys Cylinder Block Subjected to Constant and Variable Amplitude Loading Conditions Using Total Life Approach. Proceeding of the Brunei International Conference on Engineering and Technology (BICET2005), **5**:139-150.

Rahman, M.M., Ariffin, A.K., Jamaluddin, N., Haron, C.H.C., 2005g. Finite Element Based Life Prediction of Linear Generator Engine Mounting. Proceeding of the National Seminar on Computational and Experimental Mechanics (CEM-2005), p.313-321.

Reemsnyder, H.S., 1985. Simplified Stress-life Model. Bethleham Steel Corporation Report, Bethleham, PA.

Rice, S.O., 1954. Mathematical Analysis of Random Noise. Selected Papers on Noise and Stochastic Processes, Dover, New York.

Rodopoulos, C.A., Curtis, S.A., de Los Rios, E.R., SolisRomero, J., 2004. Optimisation of the fatigue resistance of 2024-T351 aluminum alloys by controlled shot peening-methodology, results and analysis. *International Journal of Fatigue*, **26**(8):849-856. [doi:10.1016/j.ijfatigue.2004.01.003]

Schaeffer, H.G., 2001. MSC.NASTRAN Primer for Linear Analysis. MSC.Software Corporation, USA.

Stephens, R.I., Fatemi, A., Stephens, R.R., Fuchs, H.O., 2001. Metal Fatigue in Engineering. John Wiley and Sons, Inc., New York, USA.

Takeuchi, H., Tamura, S., Tsunekawa, Y., Okumiya, M., 2004. Application of electrolyte jet to rapid composite electroplating. *Surface Engineering*, **20**(1):25-30. [doi:10.1179/026708404225010568]

Tomida, S., Nakata, K., 2003. Fe-Al composite layers on aluminum alloy formed by laser surface alloying with ion powder. *Surface and Coatings Technology*, **174-175**:559-563 [doi:10.1016/S0257-8972(03)00698-4]

Torres, M.A.S., Voorwald, H.J.C., 2002. An evaluation of shot peening, residual stress and stress relaxation on the fatigue life of AISI 4340 steel. *International Journal of Fatigue*, **24**(8):877-886. [doi:10.1016/S0142-1123(01)00205-5]

Tsunekawa, Y., Ueno, T., Okumiya, M., Yashiro, T., 2003. Plasma sprayed coating with water and gas atomized steel powders. *Surface Engineering*, **19**(1):17-22. [doi:10.1179/026708402225010074]

Tucker, L., Bussa, S., 1977. The SAE Cumulative Fatigue Damage Test Program: Fatigue under Complex Loading. *In*: Wetzel, R.M. (Ed.), Analysis and Experiments. SAE, Warrendale, PA, USA, p.1-54.

Vissutipitukul, P., Aizawa, T., 2005. Wear of plasma nitrided aluminum alloys. *Wear*, **259**(1-6):482-489. [doi:10.1016/j.wear.2005.02.119]

Wirsching, P.H., Paez, T.L., Oritz, K., 1995. Random Vibration, Theory and Practice. John Wiley and Sons, Inc., New York, USA.